

Fluorine NMR studies of the human carbonic anhydrase–3,5-difluorobenzenesulfonamide complex†

D. L. Veenstra and J. T. Gerig*

Department of Chemistry, University of California, Santa Barbara, California 93106, USA

Received 20 January 1998; accepted 10 February 1998

ABSTRACT: Fluorine and nitrogen-15 NMR experiments are described which show that 3,5-difluorobenzene-sulfonamide binds to human carbonic anhydrase I in a 1:1 complex, that the bound inhibitor is present as an anion and that the aromatic ring of the inhibitor undergoes rapid rotation in the complex in spite of likely interactions with the aromatic ring of Phe-91 which are strong enough to give an appreciable $^{19}\text{F}\{^1\text{H}\}$ NOE. A previously predicted enhancement of binding by fluorination of the inhibitor was confirmed. © 1998 John Wiley & Sons, Ltd.

KEYWORDS: NMR; ^{19}F NMR; carbonic anhydrase; enzyme inhibition; protein dynamics; sulfonamide; aromatic ring rotation; nuclear Overhauser effect; relaxation

INTRODUCTION

Jack Roberts' pioneering in the early 1960s provided a steady stream of examples showing how high-resolution NMR spectroscopy could provide important information about organic molecules. In the time since, NMR has become an indispensable tool for the synthetic chemist attempting to characterize newly prepared structures and rudimentary instruction in the interpretation of proton and carbon-13 NMR spectra has become part of every introductory organic chemistry course.

Most of our ideas about the conformational mobility of organic and inorganic molecules are based on NMR results. The striking abilities of NMR to provide detailed structural information and insights into molecular dynamics have not been lost on those working with proteins, nucleic acids and polysaccharides. Indeed, the first published proton NMR spectrum of a protein (taken with an 11 mM solution of ribonuclease A at 40 MHz) appeared essentially at the same time as advertisements for the venerable Varian A-60, the first commercial instrument capable of providing routine proton NMR spectra in the hands of relatively unskilled operators.

The evolution of several technologies has now made it possible to obtain multi-dimensional proton NMR spectra at frequencies in excess of 900 MHz. All of the advances in hardware and experimental design that have taken place since Roberts' path-breaking studies are necessary when applying NMR to biological

systems simply because the complexity of a protein or nucleic acid or polysaccharide is such that a standard one-dimensional spectrum is rarely able to provide much information that is directly indicative of structure or dynamics.

Contemporary NMR studies of biological structures often rely on the presence of carbon-13 and nitrogen-15 in the molecule of interest. Long before the terms coherence transfer or pulsed field gradient entered the lexicon of the biochemist, Roberts, Grant, Stothers, Lauterbur and others were collecting the essential data needed to enable the use of these isotopes in this context. However, as molecules become larger and more complex, the use of proton/deuterium/carbon-13/nitrogen-15 isotope labeling strategies to gain information about biological structure and dynamics begins to falter, primarily because spectral linewidths increase with molecular mass, eventually making it impractical to resolve and assign individual resonances.

The abilities of NMR to provide information about biological systems can be extended by application of the same paradigm that guides the use of nitroxide 'spin labels' in studies of biological systems. In the classical spin-labeling experiment, a chemically stable paramagnetic group is introduced into the system and then examined by ESR spectroscopy.¹ Because there is only one, or perhaps a few, of the paramagnetic centers present, the spectroscopic experiment does not suffer from a 'resolution' problem. Also, because the experimenter often knows the details of the chemistry that was used to place the paramagnetic center in the molecule, the 'assignment' problem is also minimized. Thus, two factors that limit the application of NMR in studies of biological systems can be overcome. However, the information that is obtainable in such a labeling experiment is limited, and is basically relevant to structure and dynamics only in the immediate vicinity of the paramagnetic species.

* Correspondence to: J. T. Gerig, Department of Chemistry, University of California, Santa Barbara, California 93106, USA.
E-mail: gerig@nmr.ucsb.edu

† Dedicated to Professor John D. Roberts on the occasion of his 80th birthday.

Contract/grant sponsor: National Institutes of Health; Contract/grant number: GM-25975.

A nuclear 'spin label' for NMR spectroscopy can, of course, be any nucleus compatible with the system of interest that produces a resolved and assignable resonance. These experiments will be easiest when the 'labeling' spins are a different type than those that are found naturally in a biopolymer and when they offer sensitivities to detection that are competitive with the ease of detecting proton NMR signals. A nucleus that fits these specifications for an NMR 'spin label' is fluorine. With few exceptions, there are no natural occurrences of fluorine in biological systems. Fluorine-19 has a natural abundance of 100% and has a sensitivity to NMR detection that is 83% that of the sensitivity of ^1H . Thus, introduction of fluorine produces a strong NMR signal that appears against a background devoid of signals from endogenous nuclei, particularly those of the solvent.

The notion of using fluorine NMR to probe molecular conformation and dynamics is another aspect of Jack Roberts' trail-blazing in NMR. He and his co-workers productively used this idea in studies of the conformations of carbocyclic compounds in the late 1960s. However, it was his Caltech colleagues, Jack Richards and his co-workers, who produced the first fluorine NMR study of a biological system.² The many advantages of the fluorine 'spin labeling' approach for NMR studies of biological systems have been recognized for more than 30 years and reviews of such studies have appeared.^{3,4}

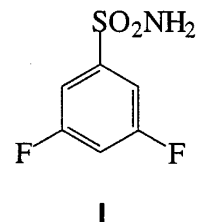
The enzyme carbonic anhydrase (CA) catalyzes the hydrolysis of carbon dioxide to carbonic acid and is present in most plant and animal tissues. Two isozymic forms, CA I and CA II, are found in human erythrocytes. They have nearly identical molecular masses (29 kDa) and each contains a zinc ion in the active site which is coordinated there to three histidines and a water molecule. The structure and function of carbonic anhydrases have been intensively investigated and the literature describing these efforts is huge. A collection edited by Dodgson *et al.*⁵ presents an overview of current research interests while Sly and Hu⁶ have reviewed the current understanding of human carbonic anhydrases.

Aromatic and heterocyclic sulfonamides are usually potent competitive inhibitors of carbonic anhydrases.⁷ A wide variety of structures have been examined for inhibitory activity and quantitative structure-activity relationships (QSARs) have been developed.⁸⁻¹⁰ The sulfonamides acetazolamide and sulfanilamide have been shown via x-ray crystallography to bind in a 1:1 complex with human carbonic anhydrase I (HCA I) and II (HCA II), with the sulfonamide group in each case replacing the water molecule at the fourth zinc coordination site.¹¹ Nitrogen-15 NMR studies have shown that benzenesulfonamide inhibitors bind to the metal ion as an anion through the nitrogen of the sulfonamide group.^{12,13}

We have previously presented fluorine NMR results demonstrating that several fluorine-substituted benzenesulfonamides bind to HCA I and HCA II with a ratio of

two inhibitor molecules per molecule of isozyme.¹⁴⁻¹⁷ Separate resonances are not observed for the two bound inhibitor molecules, indicating there is an exchange process which interconverts the protein-bound sulfonamides in the 2:1 complexes. Fluorine NMR observations show that in some cases there is slow rotation of the aromatic ring of the 2,6-difluorobenzenesulfonamide and pentafluorobenzenesulfonamide when these inhibitors are bound to HCA I.^{16,17} In contrast, tritium NMR studies have shown that in solution benzenesulfonamide binds to CA I with a 1:1 stoichiometry and that the aromatic ring of this inhibitor rapidly rotates within the enzyme-inhibitor complex.¹⁸

In an attempt to elucidate further the factors that control the stoichiometry of inhibitor binding to HCA I and the rate of rotation of the bound inhibitor aromatic ring, 3,5-difluorobenzenesulfonamide (**I**) was chosen for study. If the rate of rotation is slow in the enzyme-bound inhibitor the magnetic environments of the fluorines would likely be sufficiently different that separate resonances would be observed for the 3,5-fluorines.¹⁷ An investigation of **I** was also of interest in light of the prediction by Hansch *et al.*¹⁰ that 3,5-difluoro substitution would enhance the inhibitory power of benzenesulfonamides toward carbonic anhydrases by producing favorable hydrophobic interactions with amino acid side chains in the active site.



EXPERIMENTAL

Materials

3,5-Difluoroaniline and 4-nitrophenylacetate were purchased from Aldrich Chemical and $^{15}\text{NH}_4\text{Cl}$ (s) (99%) from MSD isotopes. The other reagents and supplies were as described previously.¹⁴ Carbonic anhydrase I (HCA I) was either isolated from hemolysate from the whole blood of DLV by following the procedure of Khalifah *et al.*¹⁹ as described previously,¹⁴ or purchased from Sigma Chemical.

3,5-Difluorobenzenesulfonamide (I). Compound **I** was synthesized by forming the corresponding sulfonyl chloride from 3,5-difluoroaniline. To 2.6 g of aniline in 7 ml of concentrated HCl and 2 ml of glacial acetic acid at -4°C was added dropwise 1.82 g of NaNO_2 in 3.6 ml of H_2O . The solution was warmed to 4°C and added to 24 ml of acetic acid saturated with SO_2 and containing 0.66 g of $\text{CuCl}_2 \cdot 2\text{H}_2\text{O}$. After 35 min at 4°C , the mixture was added to 20 ml of ice-water and extracted with diethyl ether. The ether layer was dried with sodium sulfate and then evaporated to give 6.5 g of crude product. The proton NMR spectra (CDCl_3) displayed multiplets at 7.59 and 7.20 ppm, which integrated 2:1. The upfield signal was assigned to the H-4 and the downfield signal to the H-2,6. The sulfonamide was formed by

mixing 1.1 g of crude sulfonyl chloride at 0°C with 10 ml of 58% aqueous ammonia, also at 0°C, followed by stirring for 1 h as the mixture warmed to room temperature. The solution was acidified to pH 1 with 6 M HCl, cooled and the precipitated solid was collected. Recrystallization from water gave 0.45 g (50%) of product, m.p. 165°C. The IR spectra indicated a primary sulfonamide, with absorbances at 3400 and 3300 cm⁻¹. The mass spectrum showed a parent ion at *m/z* 193. The proton spectra (CDCl₃) consisted of multiplets at 7.52 ppm (H-2,6) and 7.34 ppm (H-4) and a broad singlet at 6.9 ppm (sulfonamide protons). The fluorine-19 NMR spectrum was as expected and is described below.

3,5-Difluorobenzene[¹⁵N]sulfonamide. This was synthesized from ¹⁵NH₄Cl (Merck) and 3,5-difluorobenzenesulfonyl chloride using 1 mmol of the crude sulfonyl chloride and a twofold excess of ¹⁵NH₄Cl. Recrystallization from 80% ethanol afforded 19 mg (0.1 mmol, 10% yield) of the product, m.p. 160–165°C. Mass spectrometry gave a parent ion at *m/z* 194. The proton and fluorine-19 NMR spectra were as expected.

4-Fluorobenzenesulfonamide. This was prepared as described previously.¹⁴

Instrumentation

Melting points were determined on a Mel-Temp apparatus and are uncorrected. Routine proton NMR spectra were recorded on GN-500 and Gemini 200 spectrometers. Fluorine NMR experiments at 282 MHz were performed on a General Electric GN-300 spectrometer and those at 470 MHz on a General Electric GN-500 spectrometer. Nitrogen-15 experiments were carried out at 50.6 MHz on the GN-500 spectrometer, as described previously.¹⁴ UV-visible spectra were determined on an HP-8452 diode-array spectrometer equipped with an HP 89500 UV-visible ChemStation (Hewlett-Packard). pH measurements were made with a Markson Model 88 pH meter connected to a Fisher gel-filled electrode.

Methods

Inhibition of HCA I activity was examined by following the kinetics of the hydrolysis of 4-nitrophenyl acetate.^{20,21} A 3 mM solution of 4-nitrophenyl acetate was prepared by dissolving 54.3 mg of 4-nitrophenyl acetate in 3 ml of acetone and then slowly adding water with vigorous stirring to a final volume of 100 ml. For a typical run, appropriate volumes of 15 mM phosphate buffer at pH 7.5, 4-nitrophenyl acetate solution and enzyme were mixed to give 3 ml of a solution in which the enzyme concentration was 1.7 μM, the buffer concentration 10 mM and the 4-nitrophenyl acetate concentration 1 mM. Small aliquots of a concentrated solution of the inhibitor were added to give a final concentration of inhibitor that varied from 0.3 to 6.6 μM. The change in absorbance at 348 nm, the isosbestic point of 4-nitrophenol and 4-nitrophenolate, was determined alternately for a cuvette containing the reaction mixture and one containing the buffer with substrate only (as a reference) at 3–5 s intervals for 1–2 min. The rate of spontaneous hydrolysis of the substrate was assumed to be the same in the enzyme-containing mixture and the blank. The rate of product appearance with time was

calculated using the kinetics software package of the HP instrument.

Samples for NMR spectroscopy were contained in 10 mm tubes and were prepared by dissolving sufficient protein in 3 ml of D₂O to afford a solution approximately 1 mM. Enzyme concentrations in the NMR samples were determined by UV spectroscopy using $A_{280} = 48\,900 \text{ l mol}^{-1} \text{ cm}^{-1}$.²² The 'pD' of the NMR samples was determined using a glass electrode and ranged from 6.1 to 6.8. Aliquots of concentrated inhibitor solutions were added to the NMR samples to obtain the desired enzyme to inhibitor ratio.

Molecular modeling studies were performed on a Silicon Graphics 4D-70 or INDY workstation using QUANTA-CHARMM (Molecular Simulations) or SYBYL (Tripos) software. Coordinates for the human CA I-sulfanilamide complex were taken from Kannan *et al.*¹¹ Apparent errors in the coordinates for the sulfanilamide molecule, as noted by Hansch *et al.*,¹⁰ were corrected by an energy minimization. To create a model of the 3,5-difluorobenzenesulfonamide complex, the amino group of sulfanilamide was removed and fluorines were added at the appropriate positions. The inhibitor was bound as the anion and a covalent bond was created between the nitrogen of the inhibitor and the zinc. Hydrogens were added to all heavy atoms and the new structure was extensively energy-minimized.

RESULTS

Fluorine NMR titration studies

The fluorine NMR spectrum of 3,5-difluorobenzene-sulfonamide consists of a multiplet 56.15 ppm downfield of the resonance of the reference compound 4-fluorophenylalanine. With samples where the concentration of the sulfonamide is less than the concentration of HCA I, a single, broad resonance approximately 1.3 ppm upfield of the shift of the free inhibitor is observed when the inhibitor concentration is less than that of the enzyme. When the inhibitor is in concentration excess over the enzyme, a multiplet appears at the chemical shift of the free inhibitor, in addition to the broad resonance (Fig. 1). The free and enzyme-bound inhibitor molecules thus exchange environments at a rate that must be considerably less than about 600 s⁻¹, the chemical shift difference in Hz. Titration of the inhibitor binding to the enzyme shows that the signal for the free inhibitor appears at ratios of inhibitor to enzyme greater than unity, showing that the binding stoichiometry is one inhibitor molecule per molecule of enzyme.

Aromatic ring rotation

As illustrated in Fig. 1, separate resonances were not observed for the two fluorines of the bound inhibitor at 25°C, consistent with the conclusion that rotation of the difluoroaromatic ring in the enzyme-inhibitor

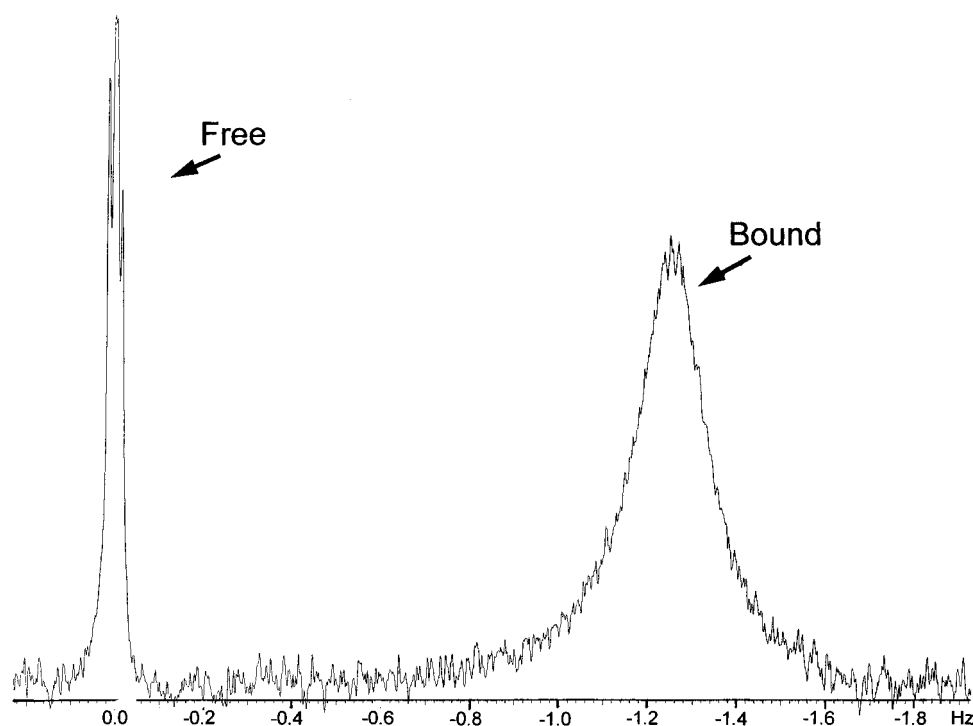


Figure 1. Fluorine NMR spectrum at 470 MHz of a sample containing human carbonic anhydrase I (0.6 mM) and 3,5-difluorobenzenesulfonamide (I, 0.9 mM) at 25 °C, 81 mM Na₂SO₄, in D₂O at 'pD' 6.5. The protein used was from the commercial (pooled) sample.

complex is rapid. The sample temperature was lowered to 4 °C in an attempt to slow rotation to the extent that resolved signals for the ring fluorine might be produced, but at the lower temperature only slight line broadening was observed. If the pentafluorobenzenesulfonamide complex (where aromatic ring rotation is slow) is a reasonable guide for the present system, a shift difference for the two environments available to the 3,5-fluorines in this complex can be estimated to be about 8 ppm,¹⁶ and our observations suggest that the rate of aromatic ring rotation must be significantly faster than 4000 s⁻¹.

The fluorine signal for the bound inhibitor is broad. At the dissociation rates for the complex estimated below there will be a negligible contribution of exchange broadening to this width.

Nitrogen-15 observations

Kanamori and Roberts¹² have shown that complexation of benzene-¹⁵N]sulfonamide to HCA I involves the anion. In their work, a 10.5 ppm upfield shift was found for the nitrogen-15 signal of the bound inhibitor relative to that of the free, neutral inhibitor. A nitrogen-15 shift of 10.3 ppm is observed for binding of 4-fluorobenzene-¹⁵N]sulfonamide to HCA I.¹⁴ The signal for HCA I-bound 3,5-difluorobenzene-¹⁵N]sulfonamide is 8.9 ppm upfield of the signal for the free inhibitor, in reasonable agreement with these previous observations and suggesting strongly that the anionic form of the

inhibitor is the bound species in this complex. Study of the binding stoichiometry of 3,5-difluorobenzenesulfonamide by means of observations of the nitrogen-15 spectra confirmed the 1:1 binding stoichiometry observed by fluorine NMR titration.

Kinetic studies

The inhibition of the HCA I-catalyzed hydrolysis of the substrate 4-nitrophenyl acetate was examined to illuminate further the nature of the interaction of sulfonamide I with this enzyme. If inhibitor binding is competitive with substrate binding, it can be shown that

$$v/v_0 = 1 - EI/E_0 \quad (1)$$

where v is the velocity of the hydrolysis reaction at a known initial concentration of substrate, S_0 , in the presence of a total concentration of inhibitor I_0 , v_0 is the velocity at the same substrate concentration in the absence of inhibitor, EI is the concentration of enzyme-inhibitor complex formed and E_0 is the total concentration of enzyme present. Should the inhibitor bind tightly to the enzyme, when the total concentration of inhibitor is low relative to the concentration of enzyme the ratio EI/E_0 can be approximated by I_0/E_0 . A plot of v/v_0 against I_0/E_0 should therefore be linear with an intercept of 1 on the v/v_0 axis and an intercept on the I_0/E_0 axis corresponding to the stoichiometry of the binding interaction. Figure 2 shows such a plot of data

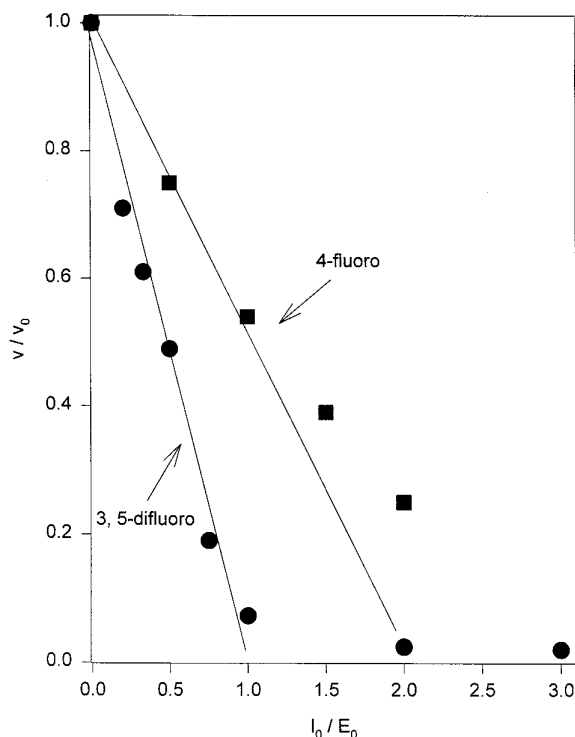


Figure 2. Inhibition of the human carbon anhydrase-catalyzed hydrolysis of 4-nitrophenyl acetate by fluorinated sulfonamide inhibitors. Extrapolation of the data for the 3,5-difluoro system to the I_0/E_0 axis indicates a 1:1 binding stoichiometry for this inhibitor, whereas a 2:1 stoichiometry for inhibition by 4-fluorobenzene-sulfonamide is suggested by the data.

for the inhibition of HCA I by 3,5-difluorobenzenesulfonamide. These results support the conclusions that binding of this sulfonamide is competitive with the substrate 4-nitrophenylacetate and that the binding interaction involves the formation of a 1:1 complex.

The measures of EI/I_0 provided by these kinetic inhibition studies permit the estimation of the dissociation constant for the enzyme-inhibitor complexes. For the 3,5-difluoro case our inhibition data indicated that the dissociation constant K_I is approximately 0.01 μM .

For comparison, Fig. 2 also shows a plot of inhibition data for 4-fluorobenzene-sulfonamide. The formation of a 2:1 inhibitor-enzyme complex in this system is suggested, a result consonant with previously reported fluorine NMR titration studies.¹⁴

Kinetics of dissociation of enzyme inhibitor complex

Saturation transfer potentially provides a means to estimate exchange rates when a system is in the slow exchange regime. Figure 3 presents the results of a typical saturation transfer experiment done with the HCA I complex of inhibitor I. Saturation of the signal corresponding to the enzyme-bound species led to a *ca.* 18% reduction in the intensity of the downfield (free inhibitor) signal. However, saturation of the free signal

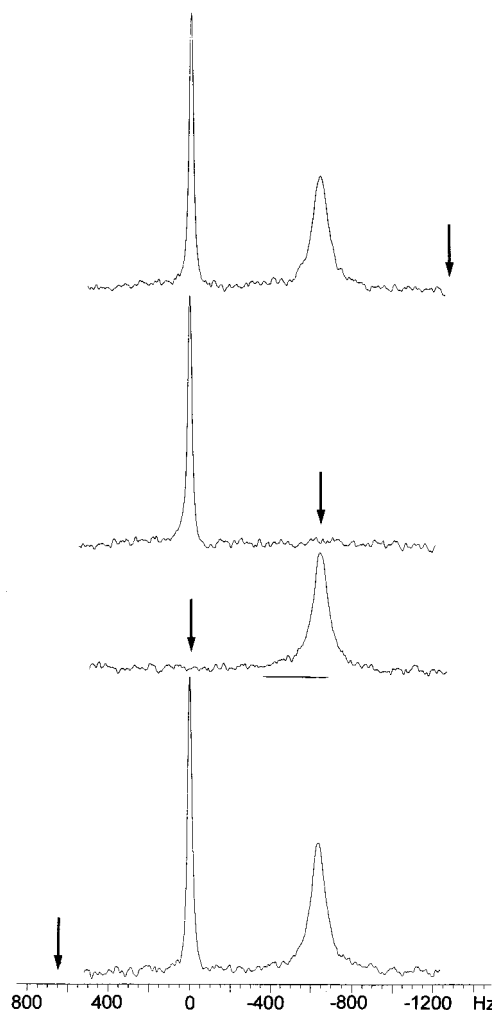


Figure 3. Results of typical saturation transfer experiments at 470 MHz carried out to determine the rate of dissociation of the 3,5-difluorobenzenesulfonamide-human carbonic anhydrase complex at 25°C. The inhibitor-enzyme concentration ratio was 2:1; the protein used for the sample was from a single source (DLV). Selective saturation at frequencies indicated by the arrows was carried out by the DANTE method;¹⁴ the top and bottom spectra are controls in which the position of irradiation is separated from the nearest peak by the chemical shift difference between the two fluorine signals of the spectrum.

produced no significant change in the intensity of the bound signal. If we assume that the inhibitor binding equilibrium can be presented by



and that the free inhibitor, represented by I_F , converts to the bound inhibitor (I_B) by a pseudo-first-order process characterized by the rate constant k_{FB} , then

$$k_{FB} = \frac{(F_0/F - 1)}{T_1^F} \quad (3)$$

where T_1^F is the spin-lattice relaxation time for the free inhibitor and F and F_0 are the observed intensities of the signal for the free species in the presence and

Table 1. Observed and calculated fluorine NMR parameters for the 3,5-difluorobenzenesulfonamide–human carbonic anhydrase I system^a

Parameter	Observed	Calculated ^b
Shift difference (ppm) ^c	1.3	—
T_1 (282) (s), 'free'	3.8	3.2
T_1 (282) (s), 'bound'	0.40	0.38
T_1 (470) (s), 'free'	1.8	2.9
T_1 (470) (s), 'bound'	0.63	0.60
$w_{1/2}$ (282) (Hz), 'bound'	20	10
$w_{1/2}$ (470) (Hz), 'bound'	56–70	19
$^{19}\text{F}\{^1\text{H}\}$ NOE (282) steady state, 'free'	−0.43	−0.28
$^{19}\text{F}\{^1\text{H}\}$ NOE (282) steady state, 'bound'	−0.82	−0.82
$^{19}\text{F}\{^1\text{H}\}$ NOE (470) steady state, 'free'	−0.25	−0.17
$^{19}\text{F}\{^1\text{H}\}$ NOE (470) steady state, 'bound'	−0.67	−0.67

^a Values observed in enzyme–inhibitor systems for which approximately 66% of the total fluorine signal intensity appeared at the chemical shift of the enzyme-bound inhibitor.

^b Calculated values obtained using the model spin system and parameters discussed in the text.

^c The fluorine signal for the enzyme-bound inhibitor is upfield from that of the free inhibitor.

absence of saturation of the bound signal, respectively. The measured T_1 for the free inhibitor in the absence of protein is 4.1 s. Hence the rate constant k_{FB} is estimated to be about 0.04 s^{-1} . No saturation transfer was detected when the free inhibitor signal was saturated. The value of k_{BF} calculated from k_{FB} and the ratio of concentrations of free and enzyme-bound inhibitor ($k_{\text{BF}} \approx 0.02 \text{ s}^{-1}$) corresponds to a half-life for dissociation of the complex of about 50 s. One can estimate that a $< 1\%$ signal intensity change for the bound signal would be expected in a saturation transfer experiment wherein the free inhibitor signal is saturated, given the observed T_1 for the bound signal of about 0.4 s^{-1} . This level of change would be difficult to detect given the noise levels in these experiments and the breadth of the fluorine signal for the bound inhibitor.

$^{19}\text{F}\{^1\text{H}\}$ NOEs

Broadband saturation of all proton signals of samples containing inhibitor I HCA I (producing a steady-state $^{19}\text{F}\{^1\text{H}\}$ NOE) led to significant reductions of the signal intensities of the fluorine signals for both the free and enzyme-bound inhibitor (Table 1). The negative NOE observed for the resonance of the free inhibitor must be the result of exchange with complexed inhibitor since the same experiment with the inhibitor in the absence of enzyme produced a small, positive $^{19}\text{F}\{^1\text{H}\}$ NOE.

The dipolar interactions which produce the observed $^{19}\text{F}\{^1\text{H}\}$ NOEs were explored by means of two-dimensional $^{19}\text{F}\{^1\text{H}\}$ NOE experiments. Typical results are shown in Fig. 4. Distinctive cross peaks are observed for the free and protein-bound inhibitors,

showing that in each case the dominant dipole–dipole interactions producing the NOEs are probably with the hydrogens of the aromatic ring of the inhibitor. For the free inhibitor, cross peaks are observed at 7.15 and 6.95 ppm, whereas in the complex the protons of the aromatic ring of the inhibitor experience an appreciable upfield shift to about 6.8 ppm.

There are faint hints at longer mixing times of the involvement of protons of enzyme at shifts of -0.5 and 0.5 ppm, in addition to other protons with shifts below 7.5 ppm. A study of the mixing time dependence of the cross peaks indicated that they arise by spin diffusion processes.

Computer modeling

To confirm the interpretations made of the various NOE experiments that were performed, we sought to create a computer model of the interaction of the proton and fluorine spins of the inhibitor with those of the enzyme. Cartesian coordinates for the hydrogens and fluorines of the aromatic ring of the free inhibitor were taken to be the same as those of 1,3-difluorobenzene.²³ The enzyme–inhibitor complex was represented for our calculations by the spins of the inhibitor's aromatic ring and the 95 amino acid hydrogens closest to the fluorines of the inhibitor (Fig. 5). Motion of the free I was characterized by a rotational correlation time ($\tau_{\text{c}, \text{I}}$) and a correlation time ($\tau_{\text{i}, \text{I}}$) for rotation about the C-1—C-4 axis. It was assumed that the collection of spins representing the complex tumbles isotropically with a correlation time $\tau_{\text{c}, \text{EI}}$. However, the aromatic ring of the inhibitor within the complex was assumed to undergo two-site jump–rotation within the binding site

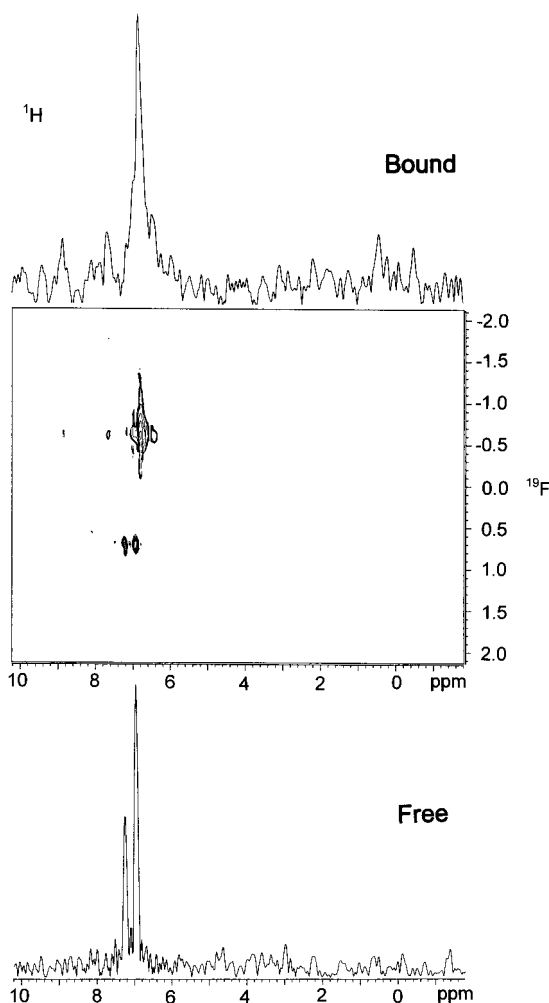


Figure 4. Results of a 2D heteronuclear $^{19}\text{F}\{^1\text{H}\}$ NOE experiment at 470 MHz and 25 °C for a sample in which the inhibitor to enzyme concentration ratio was 2 : 1 and the enzyme concentration was 0.8 mM. Transctions at the fluorine frequency of the free inhibitor (bottom) and the enzyme-bound inhibitor (top) are shown. Data were collected using the States method and a standard pulse sequence³⁰ for a total of 153 t_1 values. For each t_1 value 72 scans were collected with a relaxation delay of 10 s between scans. The mixing time for the experiment shown was 250 ms.

at a rate characterized by the residence time $\tau_{i, \text{EI}}$. Following the same procedures used in our previous calculations of a similar nature,¹⁸ relaxation behaviors for the collections of spins representing the free inhibitor and the complex were described in terms of the Solomon equations.²⁴ Spectral densities for spin pairs undergoing isotropic rotation were computed using standard equations;²⁵ spectral densities for dipolar interactions between the nuclei of the inhibitor ring and nuclei of the enzyme where jump-rotation modulates internuclear distances were calculated using equations based on the work of Tropp.²⁶ Spectral densities for interactions between the five spins on the aromatic ring of the inhibitor (jump-rotation but no change in internuclear distances) were computed using the equations given by London.²⁷ Methyl groups of both EI and E

were assumed to rotate freely, with rotation characterized by an internal correlation time of 20 ps. Spectral densities for dipolar interactions between spins of the methyl groups and other spins of the model were computed by procedures according to Olejniczak.²⁸ The chemical shift anisotropy (CSA) contribution to fluorine relaxation was computed using the parameters for 3-fluorotyrosine suggested by Hull and Sykes²⁹ and the equations of these authors. Since all experiments reported were carried out with D_2O solutions, all interactions of solvent-exchangeable hydrogens with other hydrogens of the EI and E models were calculated using the gyromagnetic ratio of deuterium. Separate calculations were performed for the two fluorines of the inhibitor and then averaged, since the rate of rotation of this ring in the complex is rapid.

It was found that the T_1 relaxation behavior of the free inhibitor at 282 and 470 MHz could be well represented by the model described when $\tau_{c, \text{I}} = 0.25$ ps and $\tau_{i, \text{I}} = 0.20$ ps. The use of values of $\tau_{c, \text{EI}} = 15$ ns and $\tau_{i, \text{EI}} = 3$ ns for the enzyme-inhibitor complex gave calculated T_1 and steady-state $^{19}\text{F}\{^1\text{H}\}$ NOEs in agreement with observations. The value of $\tau_{c, \text{EI}}$ used is in good agreement with estimates for the overall rotational correlation time of this protein¹⁸ and it therefore appears that the inhibitor molecule is bound firmly to the active site of the enzyme, having only the freedom necessary to permit rotation of its aromatic ring. Fluorine NMR data for systems where signals for both free and enzyme-bound inhibitor were present were reasonably well reproduced by calculation when these parameters, along with the value $k_{\text{FB}} = 0.13 \text{ s}^{-1}$, were used (Table 1). Calculated steady state and time-dependent NOEs were highly sensitive to the values of $\tau_{i, \text{EI}}$, and k_{FB} and it is believed that the values given for these parameters are reliably estimated to within $\pm 15\%$.

Cross-sections of 2D $^{19}\text{F}\{^1\text{H}\}$ for various mixing times were calculated using the model (Fig. 6). These are in qualitative accord with experiment. The calculations show that, owing to spin diffusion effects, at longer mixing times cross peaks from the protons of Phe-91, Gln-92, Phe-93, His-94, His-119, Ala-121, His-122, Leu-141, Val-143 and Leu-198 may appear at about the experimentally observed relative intensities, even though these spins are 0.5–1.2 nm distant from the fluorines.

The relative intensities for $^{19}\text{F}\{^1\text{H}\}$ NOE cross peaks for interactions between the protons and fluorines of the inhibitor's aromatic ring are not correctly predicted by the calculations (Fig. 6, right panels). In the model, H-4 of the phenyl ring of Phe-91 is predicted to be about 0.25 nm from one fluorine of the complex and would surely be able to produce a direct $^{19}\text{F}\{^1\text{H}\}$ NOE. If it is assumed that the shift of this proton is 6.9 ppm in the complex, the calculations (Fig. 6, left panels) show that the NOE arising from interaction of fluorine with this proton would now contribute to cross-peak intensities for both the free and bound inhibitor signals in such a way that the relative cross-peak intensities are in agreement with experiment. These calculations thus provide

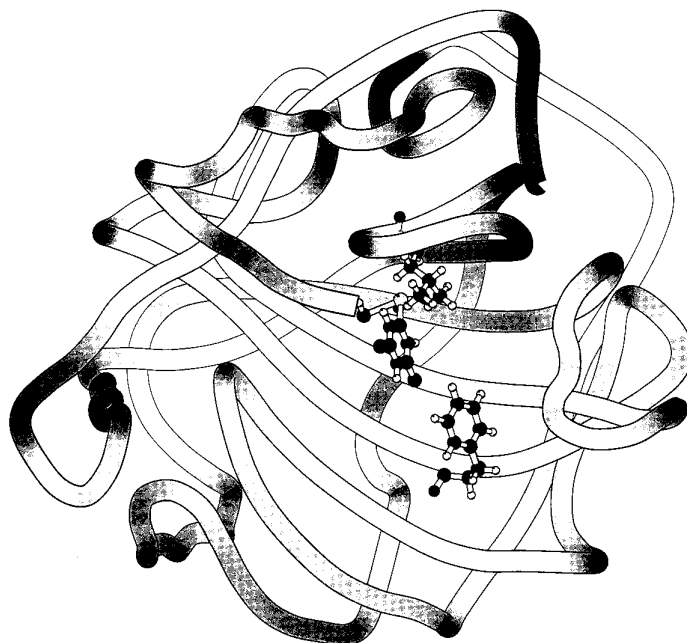


Figure 5. Representation (MOLSCRIPT³¹) of the computer model used to interpret the fluorine relaxation and NOE data for the human carbonic anhydrase complex of I. Cartesian coordinates for the 98 hydrogens closest to the fluorine nuclei were generated as described in the Experimental section.

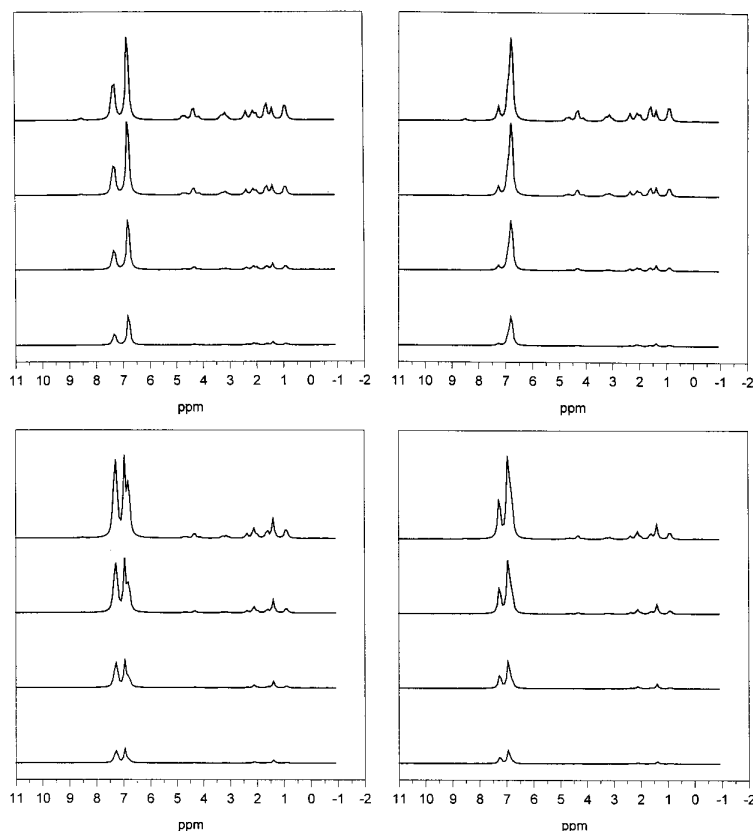


Figure 6. Calculated transections of $^{19}\text{F}\{^1\text{H}\}$ 2D NOE experiments obtained using the model system shown in Fig. 5 and the parameters indicated in the text. The protons shifts used for the amino acids of the protein were standard random coil values³² except as noted, and the shifts for the aromatic protons of the inhibitor were those observed experimentally (Fig. 5). The top panels correspond to the fluorine signal for the bound inhibitor. For the panels at the left the chemical shift of the protons of the phenyl ring of Phe-91 were set at 7.32–7.38 ppm (random coil values) whereas for the panels on the right the shifts of these protons were set at 6.9 ppm. Calculations in each series correspond to mixing times of 0.060, 0.125, 0.250 and 0.400 s. An arbitrary proton signal width of 17 Hz was used for all calculations; the conclusions reached do not depend on the value of this parameter.

some support for the conclusion that an intimate Phe-91–3,5-difluorophenyl interaction is present in the complex.

CONCLUSIONS

The NMR observations that we have described indicate that (i) the complex formed with HCA I by 3,5-difluorobenzenesulfonamide involves a single molecule of inhibitor bound to the enzyme, (ii) it is the anionic form of the inhibitor that is bound, (iii) the aromatic ring of the inhibitor rotates rapidly within the complex and (iv) contacts between the aromatic ring of the inhibitor and the aromatic ring of the Phe-91 are sufficiently strong that NOEs develop between the spins of these groups. The modeling calculations described suggest that the structure of this complex (in solution) is probably similar to that found for the sulfanilamide–HCA I complex in the crystalline state.

A quantitative structure–activity study of the inhibition of human carbonic anhydrase II reported by Hansch *et al.*¹⁰ has suggested that placement of two fluorines *meta* to the sulfonamide function should produce about an order of magnitude improvement in inhibitor binding as measured by a reduction in the dissociation constant K_i of the enzyme–inhibitor complex. Although our studies used HCA I, the change in dissociation constant for benzenesulfonamide ($K_i = 2 \times 10^{-7}$ M)¹² to the value estimated from our work for 3,5-difluorobenzenesulfonamide ($K_i \approx 1 \times 10^{-8}$ M) is consistent with this prediction. Hydrophobic interactions, particularly with Leu-198 of the active site, are apparently the source of the more effective binding by the fluorinated inhibitor to HCA II.¹⁰ Our results imply that hydrophobic interactions with Phe-91 are the primary source of the improved binding to HCA I.

There is a significant disparity between the rate of dissociation of the complex determined by saturation transfer and estimated through calculations of NOEs and relaxation effects using a reasonable model for the complex. The source(s) of this disparity is not apparent at present. It may be that the two-site model used to interpret experimental data in both cases may be too simple an assumption, or there may be a flaw in the saturation-transfer experiments that we have not detected.

We have noted small differences in the fluorine NMR spectra that arise from complexes of enzyme isolated from a single source (DLV) and from samples prepared using commercial protein which presumably contain enzymes pooled from many sources. With the genetically homogeneous protein the position of the fluorine resonance for the bound inhibitor was to slightly higher field (*ca.* 0.07 ppm) and was slightly narrower (*ca.* 10 Hz) than the signal for samples prepared with commercial protein. The origins of these differences were not explored but could arise from differences in glycosylation, deamidation or primary sequence of the enzyme. It is likely that other features of the binding, such as the

finding constant and dissociation rate, are also somewhat sensitive to these differences in protein.

Finally, we note once again that the linewidth of the fluorine signal of the bound inhibitor is significantly broader than would be expected based on the analysis of relaxation and NOE data that was carried out (Table 1).³ Excess fluorine linewidth has been observed in many systems and is often taken to imply the presence of exchange processes or protein inhomogeneity. The reasons for the increased linewidth are not yet apparent in any of these systems.

Acknowledgements

A notable aspect of Jack Robert's research has always been the involvement of able undergraduates in all of his endeavors. It is thus appropriate that most of the work described in this paper was carried out by a talented and motivated undergraduate student, J.T.G. thanks David Veenstra and Jack Roberts for their inspiring efforts during very different stages of his career.

This work was supported by Grant GM-25975 from the National Institutes of Health. D.L.V. received support from the President's Undergraduate Research Fund. We thank Jarrod A. Smith for initial molecular modeling studies of the difluorinated benzenesulfonamide–CA I complex and Adrian S. Culf for the preparation of some samples.

REFERENCES

1. L. J. Berliner and J. Reuben (Eds), *Spin-Labeling: Theory and Applications*, *Biol. Magn. Reson.* **8**, 1 (1989).
2. T. M. Spotswood, J. M. Evans and J. H. Richards, *J. Am. Chem. Soc.* **89**, 5052 (1967).
3. J. T. Gerig, *Prog. Nucl. Magn. Reson. Spectrosc.* **26**, 293 (1994).
4. M. A. Danielson and J. J. Falke, *Annu. Rev. Biophys. Biomol. Struct.* **25**, 163 (1996).
5. S. J. Dodgson, R. E. Tashian, G. Gros and N. D. Carter, *The Carbonic Anhydrases. Cellular Physiology and Molecular Genetics*. Plenum Press, New York (1991).
6. W. S. Sly and P. Y. Hu, *Annu. Rev. Biochem.* **64**, 3775 (1995).
7. T. H. Maren and G. Sanyal, *Annu. Rev. Pharmacol. Toxicol.* **23**, 439 (1983).
8. M. C. Menziani, P. G. DeBenedetti, F. Gago and W. G. Richards, *J. Med. Chem.* **32**, 951 (1989).
9. K. M. Merz, Jr and L. Banci, *J. Am. Chem. Soc.* **119**, 863 (1997).
10. C. Hansch, J. McClarin, T. Klein and R. Langridge, *Mol. Pharmacol.* **27**, 493 (1985).
11. K. K. Kannan, I. Vaara, B. Notstrand, S. Lovgren, A. Borell, K. Fridborg and M. Petef, in *Drug Action at the Molecular Level*, edited by G. C. K. Roberts. University Park Press, Baltimore (1977).
12. K. Kanamori and J. D. Roberts, *Biochemistry* **22**, 2658 (1983).
13. G. M. Blackburn, B. F. Mann, B. F. Taylor and A. F. Worrall, *Eur. J. Biochem.* **153**, 553 (1985).
14. L. B. Dugad and J. T. Gerig, *Biochemistry* **27**, 4310 (1988).
15. L. B. Dugad, C. R. Cooley and J. T. Gerig, *Biochemistry* **28**, 3955 (1989).
16. J. T. Gerig and J. M. Moses, *J. Chem. Soc., Chem. Commun.* 482 (1987).
17. A. Chang and J. T. Gerig, unpublished observations.
18. A. S. Culf, P. W. Williams and J. T. Gerig, *J. Biomol. NMR* **10**, 293 (1997).
19. R. G. Kalifah, D. J. Strader, S. H. Bryant and S. M. Gibson, *Biochemistry* **16**, 2241 (1977).
20. J. McD. Armstrong, D. V. Myers, J. A. Verpoorte and J. T. Edsall, *J. Biol. Chem.* **241**, 5137 (1966).
21. G. T. Spyridis, J. E. Meany and Y. Pocker, *J. Chem. Educ.* **62**, 1124 (1985).
22. S. Lindskog, L. E. Henderson, K. K. Kannan, A. Liljas, P. O. Nyman and B. Strandberg, in *The Enzymes*, Vol. 5, edited by P. D. Boyer, pp. 587–666. Academic Press, New York (1971).
23. S. Doraiswamy and S. D. Sharma, *J. Mol. Struct.* **102**, 81 (1983).

24. T. M. O'Connell, J. T. Gerig and P. W. Williams, *J. Am. Chem. Soc.* **115**, 3048 (1993).
25. D. Neuhaus and M. P. Williamson, *The Nuclear Overhauser Effect in Structural and Conformational Analysis*. VCH, New York (1989).
26. J. Tropp, *J. Chem. Phys.* **72**, 6035 (1980).
27. R. E. London, *Magn. Reson. Biol.* **1**, 1 (1980).
28. E. T. Olejniczak, *J. Magn. Reson.* **81**, 392 (1989).
29. W. E. Hull and B. D. Sykes, *J. Mol. Biol.* **98**, 121 (1975).
30. P. Rinaldi, *J. Am. Chem. Soc.* **105**, 5167 (1983).
31. P. J. Kraulis, *J. Appl. Crystallogr.* **24**, 946 (1991).
32. D. S. Wishart, C. G. Bigam, A. Holm, R. S. Hodges and B. D. Sykes, *J. Biomol. NMR* **5**, 67 (1995).